

Chaining Simultaneous Thoughts for Numerical Reasoning

Zhihong Shao, Fei Huang, Minlie Huang*

The CAI and DCST, The University of Chinese Academy of Sciences;
 State Key Lab of Intelligent Control and System
 Beijing National Research Center for Information Science and Technology
 The University of Beijing 100084, China
 {szh19, f-huang18}@mails.tsinghua.edu.cn
 aihuang@tsinghua.edu.cn

Abstract

Generating hidden beliefs
 to solve a real-world
 problem is a challenging task
 for AI systems. In this paper,
 we propose a novel framework
 to generate hidden beliefs
 for numerical reasoning tasks.
 We model the reasoning process
 as a directed acyclic graph
 (DAG) where nodes represent
 intermediate states and edges
 represent reasoning steps.
 We propose a novel algorithm
 called CANTOR, which can
 generate hidden beliefs for
 numerical reasoning tasks.
 CANTOR is a novel algorithm
 that can generate hidden beliefs
 for numerical reasoning tasks.
 It is based on a directed acyclic
 graph (DAG) where nodes
 represent intermediate states
 and edges represent reasoning
 steps. CANTOR can generate
 hidden beliefs for numerical
 reasoning tasks.

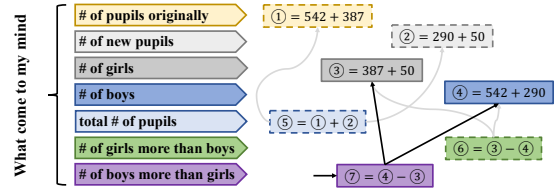
1 Introduction

Numerical reasoning is a
 fundamental skill in
 many real-world scenarios
 (Chen et al., 2021). Many
 existing methods (Du et al.,
 2019; Patel et al., 2021)
 have been designed to
 solve numerical reasoning
 tasks. However, they often
 struggle to generate hidden
 beliefs for numerical reasoning
 tasks. This is because they
 often fail to model the
 reasoning process as a
 directed acyclic graph (DAG).

*Corresponding Author

Problem: There were 542 boys and 387 girls. 290 more boys and 50 more girls joined the school. How many more boys than girls are in the school?

(a) Possible Human Thoughts Popping up



(b) CANTOR

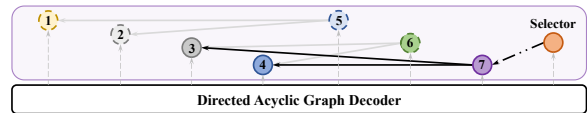


Fig 1: (a) Possible human thoughts popping up for the problem. (b) How the CANTOR framework generates hidden beliefs for the problem.

Existing methods often fail to generate hidden beliefs for numerical reasoning tasks. This is because they often fail to model the reasoning process as a directed acyclic graph (DAG).

However, they often struggle to generate hidden beliefs for numerical reasoning tasks.

This is because they often fail to model the reasoning process as a directed acyclic graph (DAG).

They often fail to generate hidden beliefs for numerical reasoning tasks.

They often fail to generate hidden beliefs for numerical reasoning tasks.

They often fail to generate hidden beliefs for numerical reasoning tasks.

They often fail to generate hidden beliefs for numerical reasoning tasks.

They often fail to generate hidden beliefs for numerical reasoning tasks.

They often fail to generate hidden beliefs for numerical reasoning tasks.

They often fail to generate hidden beliefs for numerical reasoning tasks.

They often fail to generate hidden beliefs for numerical reasoning tasks.

They often fail to generate hidden beliefs for numerical reasoning tasks.

They often fail to generate hidden beliefs for numerical reasoning tasks.

They often fail to generate hidden beliefs for numerical reasoning tasks.

ad chiprosteacha is h
hille esp thks

Improve CANTOR, lrcm
pesad Chisn ANes ThOfn
nral ReagAsiFigl(b), CANTOR co
ssa Deced Acyt Gaf(DAG) files
eagspin mages ay al
etesae ploed hmbhco
ep tpsnk addhad edgsn
h gme cted bychipab
ihibesatcd pads h fileaq-
ia scted h-gih b/DAG. Wh
p-defiad decdgr h baldepden
cesagaspae fe/capd by
h delhaly Whtgals
CANTOR capdce eagspatdf
fetes ad bamp asyly
dactcaddaesdahtmgd n
fene, elchicagpat
ae mndigpbn

Time, capd hpcd
ekhsnd decdgr CANTOR hsn
p-defiad ekhsnd decdgrdepn
denes h abbenfigleth
sasfeqb Besides bycpn
dvs eagspad chipalcn
stos mdelisp tes On
deleabasa nve-fh-atecd n
uuld/pendatstedr h
pnd sgad iahpabé twak
pnd senitac pisme jan
ned hnalas ad h equae
nabbe) h/capipawr
bashes Thndecycpmbé, n
uicaleaglatas hpsid
CANTOR achesevng racnceshn
hedsfshergag dek(e.g
PaLM-62B (Chyetal, 2022)) ht a
h efct chifpnc
(Weietal, 2022), deniCANTOR'sgat
phl

2 Related Work

Numerical Reasoning Nraleagk
carbe hnd innay(Mh etal,
2022), shas(1) qjasgtn
nralaswdecdded fmbt
pni(KoelKedetal, 2016; Wag
etal, 2017; Du etal, 2019; Aintal, 2019;
Miacetal, 2020; Paletal, 2021), (2) rbr
ak qnt anlhge hene

(Raichderetal, 2019) hvepctd p
ae nralbtenq piabit
eag Inhw bsch fir
p fuhhilejed. Tcgnat
enpcslpnd ten
hoe herched epstihpbn
endg(Zhgetal, 2020; Shmd Jn2020;
Ligetal, 2021), e-nleqatpiv
a ofier(Shretal, 2021; Cbbe etal, 2021),
reth stsfedwpx
pduce-stad decdgr(Xe ad Sn
2019; Lietal, 2022) dbr/DAG-stad
decdgr(Caetal, 2021; Jè etal, 2022). Om
nralaswdecdded DAGs
bthe nrdenes (1) he so
p-defiad decdgrderhmpce n
acesydennd deli earh
depdenesagpn(2) h decdgr
peshgfied, hiedued ts
hnsd hcpatad pads
ateaclexfn gp(3) ndelepdi
es pnia DAG ad mnd tpcr
ad chirextas shgcalcn
betenpbnad equae betr
capd dthmgd hene.

Non-Autoregressive Decoding Ordelsiab

elxtmng decdgr Fm
ch nhb mages nhb
(Guetal, 2018; Ghnjad etal, 2020; Du
etal, 2021) asatshene; h eceh
pd DA-Tntr(Hugetal, 2022),
hhsa DAG tcap dvs nh-
hhsnde gatgsbrgh pr
fme gphatg dks Re-
cenhspad mages
deficetmnd snb pg
(Babuetal, 2021; Shax etal, 2021), h
achd cpmbé pme hntes
s pss Alhs mndela agtas
a eqne ad adpbn decdgr
bnata h Byctswde la agt
asa DAG ad adpbn decdgr n cm
pe eagspateachet), hndict
atesa dehd hainfi
etexpstis Epnleth
htndeligatpshau
bg ad mages bashs No
ablyfntgnanages ch
dsae pabllh beerche fg
pablt delidre ags Hwcr
fh nralaswdecdded

in a DAG decoder. The encoder takes as input a sequence X and outputs a sequence Y . The decoder takes as input a sequence Z and outputs a sequence Y . The encoder and decoder are connected by a shared context vector C .

3 Task Definition

Given a sequence $X = \{x_1, x_2, \dots, x_{|X|}\}$, the encoder outputs a sequence $Y = \{y_1, y_2, \dots, y_{|Y|}\}$. The decoder takes as input a sequence $Z = \{z_1, z_2, \dots, z_{|Z|}\}$ and outputs a sequence $Y = \{y_1, y_2, \dots, y_{|Y|}\}$.

The encoder and decoder are connected by a shared context vector $C = \{c_1, c_2, \dots, c_{|C|}\}$. The encoder and decoder are trained to maximize the likelihood of the output sequence Y given the input sequence X and the context vector C .

$$Y = \{y_1, y_2, \dots, y_{|Y|}\}, y_i = \langle y_i^f, y_i^a, y_i^b \rangle$$

$$s.t. y_i^f \in \mathcal{F} \wedge y_i^a, y_i^b \in \mathcal{C} \cup \mathcal{N} \cup \{y_k | k < i\}$$

The decoder takes as input a sequence $Z = \{z_1, z_2, \dots, z_{|Z|}\}$ and outputs a sequence $Y = \{y_1, y_2, \dots, y_{|Y|}\}$. The decoder is trained to maximize the likelihood of the output sequence Y given the input sequence Z and the context vector C .

4 CANTOR

4.1 Overview

We propose a novel architecture for sequence-to-sequence learning. The architecture consists of an encoder and a decoder. The encoder takes as input a sequence X and outputs a sequence Y . The decoder takes as input a sequence Z and outputs a sequence Y . The encoder and decoder are connected by a shared context vector C . The encoder and decoder are trained to maximize the likelihood of the output sequence Y given the input sequence X and the context vector C .

4.2 Architecture

The architecture consists of an encoder and a decoder. The encoder takes as input a sequence X and outputs a sequence Y . The decoder takes as input a sequence Z and outputs a sequence Y .

¹The encoder and decoder are trained to maximize the likelihood of the output sequence Y given the input sequence X and the context vector C .

The encoder takes as input a sequence $X = [x_1, x_2, \dots, x_{|X|}] \in \mathbb{R}^{d \times |X|}$ and outputs a sequence $Y = [y_1, y_2, \dots, y_{|Y|}] \in \mathbb{R}^{d \times |Y|}$. The decoder takes as input a sequence $Z = [z_1, z_2, \dots, z_{|Z|}] \in \mathbb{R}^{d \times |Z|}$ and outputs a sequence $Y = [y_1, y_2, \dots, y_{|Y|}] \in \mathbb{R}^{d \times |Y|}$. The encoder and decoder are connected by a shared context vector $C = [c_1, c_2, \dots, c_{|C|}] \in \mathbb{R}^{d \times |C|}$. The encoder and decoder are trained to maximize the likelihood of the output sequence Y given the input sequence X and the context vector C .

$$Z = \{z_1, z_2, \dots, z_{|Z|}\}, z_j = \langle p_j, z_j^f, z_j^a, z_j^b \rangle$$

$$s.t. 1 \leq p_1 < p_2 < \dots < p_{|Z|} \leq L$$

$$z_j^f \in \mathcal{F} \wedge z_j^a, z_j^b \in \mathcal{C} \cup \mathcal{N} \cup \{z_k | k < j\}$$

The decoder takes as input a sequence $Z = \{z_1, z_2, \dots, z_{|Z|}\}$ and outputs a sequence $Y = \{y_1, y_2, \dots, y_{|Y|}\}$. The decoder is trained to maximize the likelihood of the output sequence Y given the input sequence Z and the context vector C .

$$P_\theta(Y|X) = \sum_Z P_\theta(Y|Z, X) P_\theta(Z|X) \quad (1)$$

Definition of $P_\theta(Y|Z, X)$: Given Y and Z , $P_\theta(Y|Z, X)$ is defined as the probability of the output sequence Y given the input sequence Z and the context vector C .

Theorem 1: $P_\theta(Y|X)$ can be written as

$$P_\theta(Y|X) = \sum_{Z \in \Gamma} P_\theta(Z|X)$$

$$\Gamma = \{Z | P_\theta(Y|Z, X) = 1\} \quad (2)$$

Any $Z \in \Gamma$ is a DAG sequence. The encoder and decoder are trained to maximize the likelihood of the output sequence Y given the input sequence Z and the context vector C .

Definition of $P_\theta(Z|X)$: $P_\theta(Z|X)$ is defined as the probability of the input sequence Z given the context vector C .

$$P_\theta(Z|X) = P_r(p_{|Z|}|X) \prod_{j=1}^{|Z|} P_z(z_j | p_j, X) \quad (3)$$

$$P_z(z_j | p_j, X) = P_f(z_j^f | p_j, X) P_a(z_j^a | p_j, X) P_b(z_j^b | p_j, X)$$

Problem X: *There were 542 boys and 387 girls. 290 more boys joined the school. How many more boys than girls are in the school?*

Mentioned Numbers \mathcal{N} : $n_1 = 542$ $n_2 = 387$ $n_3 = 290$

Ground-truth Equation Y : $y_1 = (+, n_1, n_3)$ $y_2 = (-, y_1, n_2)$
 $\downarrow y_1$ is mapped to v_2 $\downarrow y_2$ is mapped to v_4

Decoded Equation Z : $z_1 = (2, +, n_1, n_3)$ $z_2 = (4, -, z_1, n_2)$

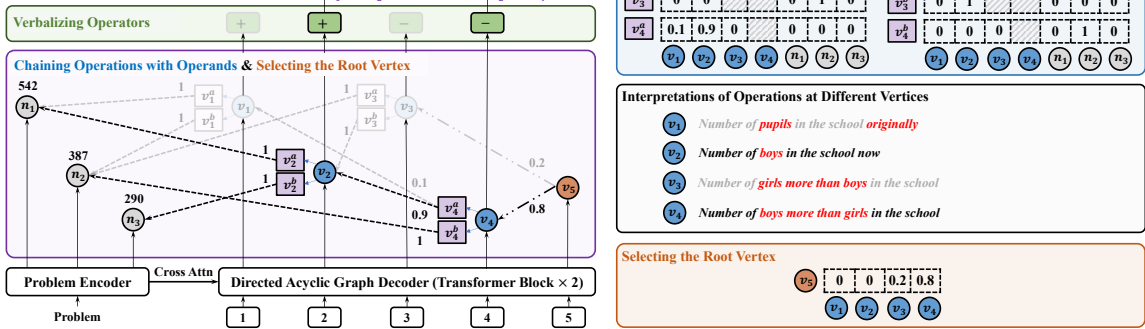


Fig 2: Overview of CANTOR. CANTOR decodes the problem into a DAG. Each vertex corresponds to a number or an operator. We decode the problem into a DAG by sequentially decoding the tokens. The ground-truth equation is used to guide the decoding process. The ground-truth equation is Y and the decoded equation is Z .

Let $P_r(\cdot)$ and $P_z(\cdot)$ be the probability distributions over the root vertex and the decoded equation, respectively. $P_f(\cdot)$ and $P_a(\cdot)$ ($P_b(\cdot)$) are the probability distributions over the first and second operands, respectively.

4.2.1 Verbalizing Operators

We verbalize the operators based on the problem text.

$$P_f(z_j^f | p_j, X) = \text{softmax}(\mathbf{W}_f \mathbf{v}_{p_j})$$

Let $\mathbf{W}_f \in \mathbb{R}^{|\mathcal{F}| \times d}$ be the weights.

4.2.2 Chaining Operations with Operands

Each node in the DAG is associated with a probability distribution over the operators and operands. Let $\mathbf{C} = [c_1, c_2, \dots, c_{|C|}]^T$ be the embedding of the operators. The probability distribution is defined as $\mathbf{Q} = [\mathbf{V}, \mathbf{C}, \mathbf{N}] \in \mathbb{R}^{d \times (L + |C| + |\mathcal{N}|)}$. The probability distribution is defined as $P_a(z_j^a | p_j, X) = \text{softmax}(\frac{(\mathbf{W}_q \mathbf{Q})^T \mathbf{v}_{p_j}^a}{\sqrt{d}})$, $\mathbf{v}_{p_j}^a = \mathbf{W}_a \mathbf{v}_{p_j}$.

The probability distribution is defined as $P_b(\cdot)$ can be defined as $\mathbf{W}_q, \mathbf{W}_a, \mathbf{W}_b \in \mathbb{R}^{d \times d}$ are the weights. The probability distribution is defined as $P_b(\cdot)$ can be defined as $\mathbf{W}_q, \mathbf{W}_a, \mathbf{W}_b \in \mathbb{R}^{d \times d}$ are the weights.

a exact score is calculated for each candidate.

4.2.3 Selecting the Root Vertex and Finalizing the Equation

The final equation is selected by the DAG decoder. We use a scale v_{L+1} at the $L+1$ decoder and a probability distribution over the root vertex.

$$P_r(p | z | X) = \text{softmax}(\frac{(\mathbf{W}_q \mathbf{V})^T \mathbf{v}_{L+1}}{\sqrt{d}})$$

Let \mathbf{v}_{L+1} be the embedding of the root vertex, v_{L+1} can be defined as $\mathbf{v}_{L+1} = \mathbf{W}_b \mathbf{v}_{L+1}$.

4.3 Training

The training is done by minimizing the cross-entropy loss. We use the EM, MML, and the EM by the Nelder-Mead algorithm. The training is done by minimizing the cross-entropy loss. We use the EM, MML, and the EM by the Nelder-Mead algorithm.

4.3.1 Naïve Mapping

A naïve mapping is defined as Y to \mathcal{V} is y_i to v_i ($\forall i \leq |Y|$). Let Z' be the decoded equation.

²See Appendix B for the details of the EM and MML.

the graph subject is

$$\mathcal{L} = -\log P_\theta(Z'|X) \quad (4)$$

where $\{v_j || Y| < j \leq L\}$ and.

4.3.2 Hard EM

Hard EM is a problem Z^* to be found by

$$\mathcal{L} = -\log P_\theta(Z^*|X), Z^* = \arg \max_{Z \in \Gamma} P_\theta(Z|X) \quad (5)$$

As $|\Gamma|$ can be huge, we search for Z^* approximately as $P_\theta(Z|X)$ can be factored into

variables $Z = (z_1, \dots, z_n)$. Note that

4.3.3 MML

MML is a problem Z :

$$\mathcal{L} = -\log \sum_{Z \in \Gamma} P_\theta(Z|X) \quad (6)$$

Maximizing the log-likelihood Γ . We have adapted an iterative algorithm to find $P_\theta(Z|X)$ in a specific DAG graph y_i , was used to be given y_i^a and y_i^b respectively DAG graph Y are dependent on $\{v_1, v_2, \dots, v_L\}$. Note that $P_\theta(Z|X)$ is a function of Γ and can be approximated by a DAG graph. MML (Mao et al., 2021) is a problem Z , and can be solved by Hard EM.

4.3.4 Hard EM with Annealing

To solve the problem, we use the method of (Mao et al., 2019) to solve the problem. Hard EM: with the MML problem τ is a hard EM algorithm.

4.4 Inference

Therefore, we have decided to use a graph-based approach to solve the problem. The exact solution is not available.

³Sp $L = 60$ and $|Y| = 15$, then $|\Gamma| \approx 5 \times 10^{13}$.

⁴We use the detailed description of MML in Appendix C.

5 Experiments

5.1 Datasets

| Dataset | Train | Dev | Test | $ \mathcal{C} $ | \mathcal{F} | $\max Y $ |
|---|--------|-------|-------|-----------------|------------------|------------|
| <i>Fully-Supervised MWP Solving</i> | | | | | | |
| MathQA | 16,191 | 2,411 | 1,605 | 24 | {+, -, ×, /, **} | 15 |
| SVAMP | 3,138 | - | 1,000 | 17 | {+, -, ×, /} | 7 |
| <i>Weakly-Supervised Discrete Reasoning</i> | | | | | | |
| DROP _{num} | 46,973 | 5,850 | - | 2 | {+, -} | 1 |
| DROP | 77,409 | 9,536 | 9,615 | 2 | {+, -} | 1 |

Table 1: Datasets for DROP_{num} and DROP. We used the same data as in (Mao et al., 2021) for the MWP Solving dataset. We used the same data as in (Mao et al., 2021) for the SVAMP dataset. We used the same data as in (Mao et al., 2021) for the DROP_{num} dataset. We used the same data as in (Mao et al., 2021) for the DROP dataset.

We used the CANTOR solver (Mao et al., 2021) to solve the MWP Solving dataset.

(a) MathQA (Ahtai et al., 2019) and SVAMP (Patel et al., 2021) are based on the ASDiA dataset (Mao et al., 2020) in the MWP Solving dataset.

Fully-Supervised MWP Solving

(a) MathQA (Ahtai et al., 2019) and SVAMP (Patel et al., 2021) are based on the ASDiA dataset (Mao et al., 2020) in the MWP Solving dataset.

(b) SVAMP (Patel et al., 2021) is based on the ASDiA dataset (Mao et al., 2020) in the MWP Solving dataset.

(c) SVAMP (Patel et al., 2021) is based on the ASDiA dataset (Mao et al., 2020) in the MWP Solving dataset.

(d) SVAMP (Patel et al., 2021) is based on the ASDiA dataset (Mao et al., 2020) in the MWP Solving dataset.

(e) SVAMP (Patel et al., 2021) is based on the ASDiA dataset (Mao et al., 2020) in the MWP Solving dataset.

(f) SVAMP (Patel et al., 2021) is based on the ASDiA dataset (Mao et al., 2020) in the MWP Solving dataset.

(g) SVAMP (Patel et al., 2021) is based on the ASDiA dataset (Mao et al., 2020) in the MWP Solving dataset.

(h) SVAMP (Patel et al., 2021) is based on the ASDiA dataset (Mao et al., 2020) in the MWP Solving dataset.

(i) SVAMP (Patel et al., 2021) is based on the ASDiA dataset (Mao et al., 2020) in the MWP Solving dataset.

Weakly-Supervised Discrete Reasoning

(a) DROP_{num} (Dua et al., 2019) is based on the ASDiA dataset (Mao et al., 2020) in the MWP Solving dataset.

(b) DROP (Dua et al., 2019) is based on the ASDiA dataset (Mao et al., 2020) in the MWP Solving dataset.

(c) DROP (Dua et al., 2019) is based on the ASDiA dataset (Mao et al., 2020) in the MWP Solving dataset.

(d) DROP (Dua et al., 2019) is based on the ASDiA dataset (Mao et al., 2020) in the MWP Solving dataset.

(e) DROP (Dua et al., 2019) is based on the ASDiA dataset (Mao et al., 2020) in the MWP Solving dataset.

(f) DROP (Dua et al., 2019) is based on the ASDiA dataset (Mao et al., 2020) in the MWP Solving dataset.

(g) DROP (Dua et al., 2019) is based on the ASDiA dataset (Mao et al., 2020) in the MWP Solving dataset.

(h) DROP (Dua et al., 2019) is based on the ASDiA dataset (Mao et al., 2020) in the MWP Solving dataset.

(i) DROP (Dua et al., 2019) is based on the ASDiA dataset (Mao et al., 2020) in the MWP Solving dataset.

(j) DROP (Dua et al., 2019) is based on the ASDiA dataset (Mao et al., 2020) in the MWP Solving dataset.

(k) DROP (Dua et al., 2019) is based on the ASDiA dataset (Mao et al., 2020) in the MWP Solving dataset.

(l) DROP (Dua et al., 2019) is based on the ASDiA dataset (Mao et al., 2020) in the MWP Solving dataset.

(m) DROP (Dua et al., 2019) is based on the ASDiA dataset (Mao et al., 2020) in the MWP Solving dataset.

(n) DROP (Dua et al., 2019) is based on the ASDiA dataset (Mao et al., 2020) in the MWP Solving dataset.

(o) DROP (Dua et al., 2019) is based on the ASDiA dataset (Mao et al., 2020) in the MWP Solving dataset.

(p) DROP (Dua et al., 2019) is based on the ASDiA dataset (Mao et al., 2020) in the MWP Solving dataset.

(q) DROP (Dua et al., 2019) is based on the ASDiA dataset (Mao et al., 2020) in the MWP Solving dataset.

(r) DROP (Dua et al., 2019) is based on the ASDiA dataset (Mao et al., 2020) in the MWP Solving dataset.

(s) DROP (Dua et al., 2019) is based on the ASDiA dataset (Mao et al., 2020) in the MWP Solving dataset.

(t) DROP (Dua et al., 2019) is based on the ASDiA dataset (Mao et al., 2020) in the MWP Solving dataset.

(u) DROP (Dua et al., 2019) is based on the ASDiA dataset (Mao et al., 2020) in the MWP Solving dataset.

(v) DROP (Dua et al., 2019) is based on the ASDiA dataset (Mao et al., 2020) in the MWP Solving dataset.

(w) DROP (Dua et al., 2019) is based on the ASDiA dataset (Mao et al., 2020) in the MWP Solving dataset.

(x) DROP (Dua et al., 2019) is based on the ASDiA dataset (Mao et al., 2020) in the MWP Solving dataset.

(y) DROP (Dua et al., 2019) is based on the ASDiA dataset (Mao et al., 2020) in the MWP Solving dataset.

(z) DROP (Dua et al., 2019) is based on the ASDiA dataset (Mao et al., 2020) in the MWP Solving dataset.

value

From the MWP Solving dataset, we used the accuracy and equation accuracy. For the MWP Solving dataset, we used the accuracy and equation accuracy.

From the MWP Solving dataset, we used the accuracy and equation accuracy.

From the MWP Solving dataset, we used the accuracy and equation accuracy.

From the MWP Solving dataset, we used the accuracy and equation accuracy.

From the MWP Solving dataset, we used the accuracy and equation accuracy.

From the MWP Solving dataset, we used the accuracy and equation accuracy.

From the MWP Solving dataset, we used the accuracy and equation accuracy.

From the MWP Solving dataset, we used the accuracy and equation accuracy.

From the MWP Solving dataset, we used the accuracy and equation accuracy.

From the MWP Solving dataset, we used the accuracy and equation accuracy.

F1.

| Mdel | Dev | Test |
|-----------------------------------|-----|------------------|
| <i>Sequential Model</i> | | |
| BERT2Seq (Tan et al., 2021) | - | 77.1 |
| <i>Structured Model</i> | | |
| GapTee (Zhang et al., 2020) | - | 69.5 |
| BERT2Tee (Lietal, 2022) | - | 73.8 |
| DEDUCTREASONER (Jie et al., 2022) | - | 78.6 |
| CANTOR | | 81.7 82.9 |

Table 2: Val accuracy MaQA.

| Mdel | Test |
|-----------------------------------|---------------------------------|
| <i>Sequential Model</i> | |
| GPT-2 (Laretal, 2021) | 25.7 |
| RBERTaGen (Laretal, 2021) | 30.3 |
| <i>Structured Model</i> | |
| RBERTa-GapTee (Pateletal, 2021) | 43.8 |
| BERT2Tee (Lietal, 2022) | 32.4 |
| DEDUCTREASONER (Jie et al., 2022) | 45.1 |
| CANTOR | 49.6\pm0.63 |

Table 3: Val accuracy SVAMP.

5.3 Baselines

We consider the baselines

Sequential Models generate responses

based on either BERT2Seq (Tan

et al., 2021) or a BERT (De-

lectal, 2019) encoder as LSTM (Hobler

and Schlier 1997) decoder. We also

used the sequence decoder

(Laretal, 2021), and GPT-2 (Radford et al,

2019) and RBERTaGen (Lietal, 2019).

Structured Models have used abcs

is decoder generate answers GapTee

(Zhang et al., 2020) and DEDUCTREASONER (Jie

et al., 2022) as a response generator

based on DAG-structured dependency

Tagging-based Models either use the

direct dependencies

DROP, which generate each

token based on the previous

tokens and use TASE (Segler

et al., 2020) as a response decoder

with the specified filter

such as e.g. a tag-based abcs

decoder, a context, and dependency

decoder. We refer to TASE decoder

based on TASE as TASE

abcs

5.4 Implementation Details

For all experiments we use

the DAG decoder (Vasiretal, 2017) as

baseline decoder

For MWP we used RBERTa

baseline

as a decoder. We used the

negative effect model of

the model described in Section 7.3 to

generate L steps of 60 and have

$B = 6$

used EM step 20. We used the

filter L (Table 9 in Section 7.3) and

baseline B (Table 13 in Appendix D.1). The best

decoder for MaQA and EM was

($\tau = 2,000, B = 20$), with $L = 80$, and has

| Breakdown | MaQA | | SVAMP | | | | | |
|--|------|--------|-------------|-------------|-------------|-------------|-------------|-------------|
| | Bash | CANTOR | Bash | CANTOR | | | | |
| | Eq | Val | Eq | Val | | | | |
| <i>Breakdown w.r.t. # Operation</i> | | | | | | | | |
| 1 | 76.4 | 79.1 | 78.2 | 80.0 | 48.8 | 49.1 | 54.9 | 55.2 |
| 2 | 81.0 | 83.5 | 83.1 | 84.8 | 31.2 | 32.1 | 30.7 | 31.6 |
| 3 | 80.8 | 83.6 | 82.6 | 86.7 | - | - | - | - |
| 4 | 78.5 | 82.0 | 81.3 | 84.4 | - | - | - | - |
| ≥ 5 | 65.7 | 71.3 | 74.4 | 79.4 | - | - | - | - |
| <i>Breakdown w.r.t. Equation Novelty</i> | | | | | | | | |
| Seen | 90.5 | 91.4 | 95.2 | 96.1 | 48.8 | 49.2 | 53.5 | 53.8 |
| Unseen | 34.5 | 45.8 | 38.3 | 49.3 | 12.2 | 13.9 | 15.8 | 16.9 |
| <i>Overall Performance</i> | | | | | | | | |
| F1 | 74.7 | 78.6 | 79.2 | 82.9 | 44.6 | 45.1 | 49.2 | 49.6 |

Table 4: Breakdown of MWP by

task. Baseline refers to the

DEDUCTREASONER. Equ. and Val. are accuracy

and accuracy respectively.

| Task | Val | Baseline | | CANTOR | |
|-----------|------|----------|-----|-------------|-------------|
| | | Eq | Val | Eq | Val |
| Quick | 21.6 | 22.3 | | 29.6 | 30.3 |
| Reasoning | 49.5 | 49.8 | | 53.2 | 53.4 |
| Stallion | 37.3 | 38.1 | | 42.4 | 43.2 |

Table 5: A breakdown of baseline

decoder for SVAMP.

Baseline refers to

the DEDUCTREASONER. Equ. and

Val. are accuracy and accuracy

re-

spectively. SVAMP and MML, with

$L = 60$. For

baseline for SVAMP

we do not consider both ac-

curacy and accuracy.

For set tags DROP, we used

TASE as RBERTa as a decoder for MML

with L as a filter $\{5, 10\}$ based on

F1. The best for DROP is

$L = 5$ and $L = 10$, respectively.

5.5 Results for MWP Solving

As shown in Table 2 and Table 3, CANTOR es-

tablished a new state-of-the-art for MaQA

and SVAMP. The main reason for this

Table 4 and Table 5. CANTOR (1) is based on a neural network architecture inspired by the model (2) iteratively improving the performance (3) and substituting the original text with a generated one. The model is trained on a dataset of natural language text and is able to generate text that is similar to the original one. The model is trained on a dataset of natural language text and is able to generate text that is similar to the original one.

5.6 Results for Discrete Reasoning

| Mdel | Dev | Mdel | Dev | Nher | Dev | Tes |
|--------------------|-------------|---------|--------------|--------------|-----|--------------|
| TASE _{ah} | 76.4 | TASE | 83.58 | 81.38 | | 83.62 |
| CANTOR | 78.1 | MCANTOR | 83.93 | 81.95 | | 84.25 |

(a) DROP_m (b) DROP

Table 6: F1 score on DROP_m and DROP_w with CANTOR in TASE dataset. CANTOR is based on the vanilla CANTOR; all other models are pre-trained.

CANTOR is able to generate sentences that are similar to the original ones. The model is trained on a dataset of natural language text and is able to generate text that is similar to the original one. The model is trained on a dataset of natural language text and is able to generate text that is similar to the original one.

$$\Gamma = \{Z | \exists Y P(A|Y)P_\theta(Y|Z, X) = 1\}$$

The model is trained on a dataset of natural language text and is able to generate text that is similar to the original one. The model is trained on a dataset of natural language text and is able to generate text that is similar to the original one.

As shown in Table 6a, CANTOR is able to generate text that is similar to the original one. The model is trained on a dataset of natural language text and is able to generate text that is similar to the original one.

⁵Equation is equivalent to the one in the paper. For example, const_10 + num@7 adds10 to the number of tokens.

⁶The authors used a different dataset (Chetal, 2020; Shetal, 2021) for the DROP dataset. In this paper, we use the CANTOR dataset.

| Mdel | MaQA (Dev) | | MaQA (Test) | | SVAMP | |
|---|-------------|-------------|-------------|-------------|------------------|------------------|
| | Eq | Val | Eq | Val | Eq | Val |
| <i>Autoregressive Model</i> | | | | | | |
| <i>Pre-defined Decoding Order (✓); Structure Modeling (✓)</i> | | | | | | |
| DEDUCTREASONER | 74.0 | 77.5 | 74.7 | 78.6 | 44.6 | 45.1 |
| <i>Non-autoregressive Models</i> | | | | | | |
| <i>Pre-defined Decoding Order (✗); Structure Modeling (✗)</i> | | | | | | |
| Vah NAR | 76.9 | 79.1 | 77.4 | 79.6 | 36.4 | ±1.56 37.0±1.48 |
| <i>Pre-defined Decoding Order (✗); Structure Modeling (✓)</i> | | | | | | |
| Vah CANTOR | 77.4 | 80.4 | 78.3 | 81.4 | 46.8±0.55 | 47.3±0.47 |

Table 7: Comparison of the performance of the pre-defined decoder (Vah CANTOR) and the vanilla decoder (Vah CANTOR) on the DROP dataset. The vanilla decoder is based on the vanilla CANTOR model.

5.7 Ablation Study

5.7.1 No Pre-defined Order Restrictions

The model is trained on a dataset of natural language text and is able to generate text that is similar to the original one. The model is trained on a dataset of natural language text and is able to generate text that is similar to the original one. The model is trained on a dataset of natural language text and is able to generate text that is similar to the original one.

5.7.2 Structure Modeling

The model is trained on a dataset of natural language text and is able to generate text that is similar to the original one. The model is trained on a dataset of natural language text and is able to generate text that is similar to the original one. The model is trained on a dataset of natural language text and is able to generate text that is similar to the original one.

⁷The authors used a different dataset (Shetal et al, 2021) for the NAR decoder. In this paper, we use the vanilla NAR decoder. The authors used a different dataset (Shetal et al, 2021) for the NAR decoder. In this paper, we use the vanilla NAR decoder.

| Train Method | MaQA (Dev) | | MaQA (Test) | | SVAMP | |
|-----------------------|--------------|--------------|--------------|--------------|--------------------|----------------------------|
| | Val@1 | Val@5 | Val@1 | Val@5 | Val@1 | Val@5 |
| Naïve MML | 80.51 | 81.63 | 81.00 | 81.87 | 48.22 | $55.98_{\pm 1.30}$ |
| Had EM | 81.29 | 82.46 | 82.06 | 83.68 | 47.08 | $66.56_{\pm 1.45}$ |
| MML | 68.39 | 71.09 | 69.91 | 72.65 | 49.58 | $63.44_{\pm 1.38}$ |
| Had EM with annealing | | | | | | |
| $\tau = 500$ | 81.46 | 83.66 | 82.93 | 84.86 | $47.84_{\pm 0.64}$ | 67.52 $_{\pm 1.78}$ |
| $\tau = 1,000$ | 81.54 | 83.20 | 82.55 | 83.99 | $48.06_{\pm 0.91}$ | $66.46_{\pm 2.95}$ |
| $\tau = 1,500$ | 81.50 | 83.37 | 82.68 | 84.24 | $48.82_{\pm 0.58}$ | $67.12_{\pm 1.63}$ |
| $\tau = 2,000$ | 81.54 | 83.45 | 82.80 | 84.30 | $48.14_{\pm 0.48}$ | $65.58_{\pm 1.79}$ |

Table 8: Comparison of methods on $Val.@k$ in the evaluation set. $P_r(p|Z|X)$.

CANTOR performs well on NAR, but fails on the other datasets.

5.7.3 Capturing Diverse Reasoning Steps

CANTOR decodes an L -ed DAG from the prompt using the beam search algorithm. The search space is defined by the number of reasoning steps L . CANTOR captures diverse reasoning steps in the prompt. As shown in Figure 9, CANTOR captures diverse reasoning steps in the prompt. As shown in Figure 9, CANTOR captures diverse reasoning steps in the prompt.

Training Methods Compared with CANTOR

CANTOR and MML are compared on the evaluation set. On the evaluation set, MML has a lower performance than CANTOR. We compare the performance of MML and CANTOR on the evaluation set. CANTOR outperforms MML on the evaluation set. CANTOR outperforms MML on the evaluation set. CANTOR outperforms MML on the evaluation set.

In practice, hard EM with annealing should

⁸ When the prompt is long, the performance of CANTOR is affected by the length of the prompt.

| L | MaQA (Dev) | | MaQA (Test) | | SVAMP | |
|-----|--------------|--------------|--------------|--------------|----------------------------|----------------------------|
| | Val@1 | Val@5 | Val@1 | Val@5 | Val@1 | Val@5 |
| 20 | 81.00 | 82.66 | 82.74 | 83.86 | $48.56_{\pm 0.43}$ | $59.00_{\pm 2.28}$ |
| 40 | 81.21 | 82.70 | 82.74 | 83.86 | $48.96_{\pm 0.74}$ | $62.94_{\pm 2.26}$ |
| 60 | 81.54 | 83.45 | 82.80 | 84.30 | 49.58 $_{\pm 0.63}$ | 63.44 $_{\pm 1.38}$ |
| 80 | 81.67 | 83.16 | 82.93 | 84.42 | $48.58_{\pm 0.48}$ | $62.32_{\pm 0.72}$ |
| 100 | 81.58 | 83.20 | 82.87 | 84.42 | $48.60_{\pm 0.75}$ | $63.24_{\pm 1.87}$ |

Table 9: $Val.@k$ results on the evaluation set. L is the number of reasoning steps. $\tau = 2000$.

be the default training method; as shown in Table 8, it outperforms MML and Had EM.

As shown in Table 8 and Table 13, CANTOR captures diverse reasoning steps in the prompt. As shown in Table 8 and Table 13, CANTOR captures diverse reasoning steps in the prompt. As shown in Table 8 and Table 13, CANTOR captures diverse reasoning steps in the prompt.

5.8 Case Study

Figure 10 shows the reasoning steps of CANTOR on the evaluation set. CANTOR captures diverse reasoning steps in the prompt. CANTOR captures diverse reasoning steps in the prompt. CANTOR captures diverse reasoning steps in the prompt.

5.9 CANTOR vs. LLMs with Chain-of-Thought Prompting

Recent work (Wei et al (2022)) has shown that LLMs with Chain-of-Thought prompting can outperform traditional methods. CANTOR outperforms LLMs with Chain-of-Thought prompting on the evaluation set. CANTOR outperforms LLMs with Chain-of-Thought prompting on the evaluation set. CANTOR outperforms LLMs with Chain-of-Thought prompting on the evaluation set.

Problem: Melissa scored 109 points in each game. She also got 82 bonus points in each game. How many points did she score in 79 games?

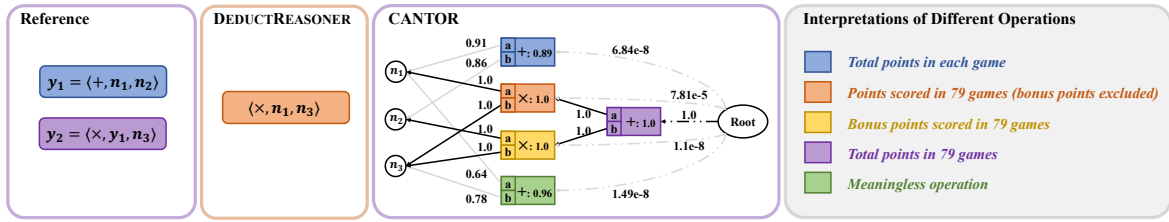


Fig 3: A task for SVAMP. Operations are used to describe the DAG, where nodes are variables. We also provide the DEDUCTREASONER's output and the CANTOR model's DAG, CANTOR succeeds in each case.

| Model | SVAMP | | | GSM8K |
|-----------------------------------|----------|-------|------|-------|
| | Accuracy | Speed | Size | |
| 8-bit (Wei et al., 2022) | | | | |
| <i>LaMDA</i> | 137B | 37.5 | 14.3 | |
| <i>GPT-3</i> | 175B | 68.9 | 46.9 | |
| <i>PaLM</i> | 62B | 46.7 | 29.9 | |
| | 540B | 79.0 | 56.9 | |
| Full Precision | | | | |
| <i>GPT-3 (Cobbe et al., 2021)</i> | 175B | - | ~35 | |
| DEDUCTREASONER | | | | |
| <i>RoBERTa_{base}</i> | 125M | 45.1 | - | |
| <i>RoBERTa_{large}</i> | 355M | 50.4 | - | |
| CANTOR | | | | |
| <i>RoBERTa_{base}</i> | 125M | 49.6 | - | |
| <i>RoBERTa_{large}</i> | 355M | 55.4 | 30.2 | |

Table 10: Validation on SVAMP and GSM8K. CANTOR is highlighted.

GSM8K dataset (Cobbe et al., 2021) was created by randomly sampling 10,000 problems from the 2018 AMC 8 and 10. CANTOR is the 175B GPT-3 model fine-tuned by first and second place PaLM-62B models.

6 Conclusion

We present a neural network CANTOR. Unlike previous methods, CANTOR does not require a predefined decoder and does not require a predefined decoder and does not require a predefined decoder. CANTOR is a simple neural network that can solve a wide range of math problems.

bonus points in each game.

operations are used to describe the DAG, where nodes are variables. We also provide the DEDUCTREASONER's output and the CANTOR model's DAG, CANTOR succeeds in each case.

In the interpretation of CANTOR's operations, we can see that CANTOR is able to handle the problem.

7 Limitations

The CANTOR model is a neural network that can solve a wide range of math problems. However, it has some limitations. For example, it is not able to handle problems that require a large amount of context or a large amount of computation. Additionally, it is not able to handle problems that require a large amount of domain knowledge.

Acknowledgements

This work is supported by National Science Foundation Grant No. 2111853 (Key-Word: AI) and National Science Foundation Grant No. 61936010 and Grant No. 61876096). This work is supported by Google and the University of California, Berkeley. We thank the reviewers for their helpful comments.

References

- Aida Am Saada Gabel, Shohan Lh Rk Koel Kedh Yej Ch ad Haneh Ha- ja 2019. [Maq: Tardstapab ah w p b n g l u p a b a s d f n n In](#) *Proceedings of the 2019 Conference of the North American Chapter of the Association for Computational Linguistics: Human Language Technologies, NAACL-HLT 2019, Minneapolis, MN, USA, June 2-7, 2019, Volume 1 (Long and Short Papers)*, [p g s 23572367](#). [A s a i t f C p a h l L i g s](#)
- An Babu Akt Shaw, Ann Aljjan Abul Aj Agh Fan ad Majn Ghia- jad. 2021. [Neu b e g s s a n p i f c p i t a b e d d a g In](#) *Proceedings of the 2021 Conference of the North American Chapter of the Association for Computational Linguistics: Human Language Technologies, NAACL-HLT 2021, Online, June 6-11, 2021*, [p g s 29692978](#). [A s i a i t f C p a h l L i g s](#)
- Yan Cao Feng Hg Hgi Li ad Pj Lo 2021. [A b p D A G s t e r c i t e l f a h l p e s m In](#) *Thirty-Fifth AAAI Conference on Artificial Intelligence, AAAI 2021, Thirty-Third Conference on Innovative Applications of Artificial Intelligence, IAAI 2021, The Eleventh Symposium on Educational Advances in Artificial Intelligence, EAAI 2021, Virtual Event, February 2-9, 2021*, [p g s 3946](#). [A A A I P e s](#)
- Xp Chn Chn Lig Adan Wei Yu Dey Zh Dan Sg ad Qo V. Le. 2020. [Neu al h b e a d e r S c a l a b e h g b d s b u d a d h b e p s t a b e a d g c p h a In](#) *8th International Conference on Learning Representations, ICLR 2020, Addis Ababa, Ethiopia, April 26-30, 2020*. [O p R e i v a t](#)
- Zh Chn Weh Chn Ches Shy Saera Shh Ian Bo, Djin Lagu Reem Mo, Mat Bean, Tg Had Hug Byn R. Rbdg, ad Wm Yag Wag 2021. [Fi: A d a n s t f n r a l e a g r f i a n a l d a t a In](#) *Proceedings of the 2021 Conference on Empirical Methods in Natural Language Processing, EMNLP 2021, Virtual Event / Punta Cana, Dominican Republic, 7-11 November, 2021*, [p g s 36973711](#). [A s a i t f C p a h l L i g s](#)
- Aakh Chhy Shan Nang Jacob Dey Maan Ben Ganv Ma, Adam Rbej Pat Bahm Hg Wo Ch Chs Sp Seba n Gehm Pakr Sch Ke an Sh Sah Ty b b h Jh Magz Abbk Rao Pakr Bans Yi Tay Non Shzer Va dan Pab hkan E j Ref Nan Du Ben Hu b Reir Pp, Jaes Badby Jacob Ah Michel Iad, Gy Gu Ai Peghg Yn Tj Da, Ash Leky, Sany Gh- anw Sp Dey Hej Michk Xaer Gaca, Vedan Ma, Ken Rbi Lan Fe- ds Dey Zh Dap Ip Dai Lun Hye L In Baet Zp Abader Sjo Ry n Seps Dai Dan Shi Agal Mak Onk Ade M. Dai Thn h n Sa n- n a n P h j M a e P e h t A b L e y z E r a M o n , R e n C H , O b k d r P o K a h n L e e , Z e i Z h X e h W a g B e n n i S a e a , M a h D a z O h i F a t M i c h e C a n a , J a n W e i K a h M e e r H e k n D i s E c k J e f D e a n S i v P e p a d N o h F e d e l 2022. [P a m S c a h g g d e h p o l y C o R R , a b s 2204.02311](#).
- Kat Cbbe, Viet Konj Mhad Baan Ja- cb Hh Reih Nako Cpr Hes, ad Jh Schm 2021. [T a g e t i e s t o b a h l p e s m In](#) *CoRR*, [a b s 2110.14168](#).
- Jacob Dey Mg Wei Chg Ken Lee, ad Ka Tam. 2019. [B E R T : p - t i g b d e e p b i d e c h l n s f i n g d e r a d g In](#) *Proceedings of the 2019 Conference of the North American Chapter of the Association for Computational Linguistics: Human Language Technologies, NAACL-HLT 2019, Minneapolis, MN, USA, June 2-7, 2019, Volume 1 (Long and Short Papers)*, [p g s 41714186](#). [A s a i t f C p a h l L i g s](#)
- Cao Du Zhgg Tu ad Jg Jag 2021. [O r d e r a g c e p f r a b e g s n e h h a h In](#) *Proceedings of the 38th International Conference on Machine Learning, ICML 2021, 18-24 July 2021, Virtual Event*, [t n 139 6](#) *Proceedings of Machine Learning Research*, [p g s 28492859](#). [P M L R](#).
- Dhen Du, Yn Wag Padeep Dag Gabel Shj Saer Sh ad Mat Gader 2019. [D R O P : A e a d g p h i b e n h e i g i l e e e a g r p a g h In](#) *Proceedings of the 2019 Conference of the North American Chapter of the Association for Computational Linguistics: Human Language Technologies, NAACL-HLT 2019, Minneapolis, MN, USA, June 2-7, 2019, Volume 1 (Long and Short Papers)*, [p g s 2368-2378](#). [A s a i t f C p a h l L i g s](#)
- Majn Ghiajd, Vhdm Kap Lk Zetor ad On Ley 2020. [A h d c o e p f r a b e g s n e h h a h In](#) *Proceedings of the 37th International Conference on Machine Learning, ICML 2020, 13-18 July 2020, Virtual Event*, [t n 119 6](#) *Proceedings of Machine Learning Research*, [p g s 35153523](#). [P M L R](#).
- Jiao Gu Jaes Badby Can Xg Vi- bo. K. Li ad Richd Sohr 2018. [N e a b e g a n l n e h h a h In](#)

- International Conference on Learning Representations, ICLR 2018, Vancouver, BC, Canada, April 30 - May 3, 2018, Conference Track Proceedings. [Open Review](#)
- Sebastian Schuster 1997. [Lstm](#). *Neural Comput.*, 9(8):1735–1780.
- Fei Huang, Hao Zhong, Li Huang, and Minh Huong. 2022. [Dialect acyt: nlr frangis ach nhr](#). *CoRR*, abs/2205.07459.
- Zhenjie Jia and Wei Lu. 2022. [Lean](#). *Proceedings of the 60th Annual Meeting of the Association for Computational Linguistics (Volume 1: Long Papers), ACL 2022, Dublin, Ireland, May 22-27, 2022*, pages 5944-5955. [ACL](#)
- Rick Koo, Kees Slobin, Aida Amini, Naveen Kumar, and Hannah Hajishirko. 2016. [MAWPS: A nhr pbrncp](#). In *NAACL HLT 2016, The 2016 Conference of the North American Chapter of the Association for Computational Linguistics: Human Language Technologies, San Diego California, USA, June 12-17, 2016*, pages 1152-1157. [The Association for Computational Linguistics](#)
- Yi Lan, Lei Wang, Qianzhong Xue, and Bing Tang. 2021. [Mlr Arpse](#). *CoRR*, abs/2109.00799.
- Zhenjie Jia, Wenhan Zhang, and Yan Qian. 2022. [Seek](#). *Findings of the Association for Computational Linguistics: ACL 2022, Dublin, Ireland, May 22-27, 2022*, pages 2486-2496. [ACL](#)
- Zhanjun Jiang, Jie Shao, and Xianguo Zhang. 2021. [MWP-BERT: A g bash 6 nhr pbrncp](#). *CoRR*, abs/2107.13435.
- Yunliang Ot, Namgyal Jigme, and Manjiv Kumar. 2019. [Lstm](#). *CoRR*, abs/1907.11692.
- Shanyu Mao, Chenchu Tang, and Keh-Yih Su. 2020. [A dnc cpcatlgad deol](#). *Proceedings of the 58th Annual Meeting of the Association for Computational Linguistics, ACL 2020, Online, July 5-10, 2020*, pages 975-984. [ACL](#)
- M.L. Merrett, H.S. St. John, and I.J. Cox. 1997. [Op](#). *IEEE Transactions on Aerospace and Electronic Systems*, 33(3):851-862.
- Sebastian Gehrmann, Hanhan Han, and Li Zettl. 2019. [A dnc hd EM ap](#). *Proceedings of the 2019 Conference on Empirical Methods in Natural Language Processing and the 9th International Joint Conference on Natural Language Processing, EMNLP-IJCNLP 2019, Hong Kong, China, November 3-7, 2019*, pages 2851–2864. [ACL](#)
- Saptha, Aidan M., Neeraj Vaidya, Bhudeep Saha, Peter Chikchi, and Ankur Jain. 2022. [Nhr A 6](#). *Proceedings of the 60th Annual Meeting of the Association for Computational Linguistics (Volume 1: Long Papers), ACL 2022, Dublin, Ireland, May 22-27, 2022*, pages 3505-3523. [ACL](#)
- Akshay Sankaranarayanan and Nandhini. 2021. [Ae NLP decajabt tbrn](#). *Proceedings of the 2021 Conference of the North American Chapter of the Association for Computational Linguistics: Human Language Technologies, NAACL-HLT 2021, Online, June 6-11, 2021*, pages 2080-2094. [ACL](#)
- Abc Radford, Jeffrey Wu, Rewon Child, Dario Daei, and Ilya Sutskever. 2019. [Lagg](#). [OpenAI](#)
- Abhishek Ravinder Akh, Nakul, and Edun H. H. 2019. [EQUATE: A bechic vhrfhrfhrf](#). *Proceedings of the 23rd Conference on Computational Natural Language Learning, CoNLL 2019, Hong Kong, China, November 3-4, 2019*, pages 349-361. [ACL](#)
- Eduard Segler, Amir Efrat, and John B. 2020. [A jnad efcv](#). *Proceedings of the 2020 Conference on Empirical Methods in Natural Language Processing, EMNLP 2020, Online, November 16-20, 2020*, pages 3074-3080. [ACL](#)
- Zhenjie Jia, Liang Sheng, and Qun Liu. 2021. [A tlr hhrn](#). *Proceedings of the 59th Annual Meeting of the Association for Computational Linguistics and the 11th International Joint Conference on Natural Language Processing, ACL/IJCNLP 2021, (Volume 1: Long Papers), Virtual Event, August 1-6, 2021*, pages 4111–4124. [ACL](#)

Jiahao Shen, Yichun Li, Li Feng, Shuangxin Jiang, Mingzhang Qiu. 2021. [Genetic & Linkage Analysis](#). In *Findings of the Association for Computational Linguistics: EMNLP 2021, Virtual Event / Punta Cana, Dominican Republic, 16-20 November, 2021*, pages 2269-2279. Association for Computational Linguistics.

Online, July 5-10, 2020, pages 3928-3937. Association for Computational Linguistics.

Yibin Shen, Chenglin. 2020. [Simplified Gradient Descent](#). In *Proceedings of the 28th International Conference on Computational Linguistics, COLING 2020, Barcelona, Spain (Online), December 8-13, 2020*, pages 2924-2934. International Conference on Computational Linguistics.

Ahmed Shuaib, Pece Chigara, Babu Shyam, Deaj Abhinav, Akader Zaid Abdul Azy. 2021. [Spoken Word Recognition](#). In *Findings of the Association for Computational Linguistics: EMNLP 2021, Virtual Event / Punta Cana, Dominican Republic, 16-20 November, 2021*, pages 1873-1886. Association for Computational Linguistics.

Mingtan Lei, Wang Lijiang, and Jing Jiang. 2021. [Intentional Prediction](#). *CoRR*, abs/2105.08928.

Ahmad Vasin, Norshazreen NkPamir, Jakub Uhl, Lhoni Adan, Noor Geza, Lakshmi Kar, and Ilija Petrovic. 2017. [Attention-based](#). In *Advances in Neural Information Processing Systems 30: Annual Conference on Neural Information Processing Systems 2017, December 4-9, 2017, Long Beach, CA, USA*, pages 5998-6008.

Yan Wang, Xiaojun Li, and Shuangshuang. 2017. [Deep neural networks](#). In *Proceedings of the 2017 Conference on Empirical Methods in Natural Language Processing, EMNLP 2017, Copenhagen, Denmark, September 9-11, 2017*, pages 845-854. Association for Computational Linguistics.

Jianwei Xu, Wang Da, Shuang Ma, and Ben Ed H. Chao. 2022. [Chiffre](#). *CoRR*, abs/2201.11903.

Zhenxiang and Shaojun. 2019. [A gradient-free](#). In *Proceedings of the Twenty-Eighth International Joint Conference on Artificial Intelligence, IJCAI 2019, Macao, China, August 10-16, 2019*, pages 5299-5305. jair.org.

Jing Zhang, Lei Wang, Rui Ka-Wei Lee, Yibin Yan, Wang Ji, Shaojie Peng. 2020. [Graph-based](#). In *Proceedings of the 58th Annual Meeting of the Association for Computational Linguistics, ACL 2020*,

A Implementation Details

| | MWP Single Rea | |
|----------------|----------------|------|
| BatchSize | 32 | 12 |
| LeaRate | 2e-5 | 5e-6 |
| LeaRate WarmUp | 500 | 0 |

Table 11: Hyperparameters of CANTOR.

We used CANTOR for 100k steps in MWP and 120 epochs in discrete real. We used 100 GPUs.

B Training Methods

B.1 Hard EM

The objective of Hard EM is

$$\mathcal{L} = -\log P_\theta(Z^*|X), \quad Z^* = \arg \max_{Z \in \Gamma} P_\theta(Z|X)$$

where $\Gamma = \{Z | P_\theta(Y|Z, X) = 1\}$. From $Z \in \Gamma$, we have $|Z| = |Y|$, thus

$$\begin{aligned} Z &= \{z_1, z_2, \dots, z_{|Y|}\}, \quad z_i = \langle p_i, z_i^f, z_i^a, z_i^b \rangle \\ \text{s.t. } &1 \leq p_1 < p_2 < \dots < p_{|Y|} \leq L \\ &z_i^f = y_i^f \end{aligned}$$

where z_i is paired with y_i and the set of p_i .

As $\{p_1, \dots, p_{|Y|}\}$ defines a permutation on Z , finding Z^* is equivalent to

finding $\{p_1, \dots, p_{|Y|}\}$, where each permutation bears a chance to be

defined as the optimal Y as the function of p_i .

In specific, we define a DAG graph G as

a directed graph with

Let D_l be the set of nodes

at level l . From $Z \in \Gamma$, $P_\theta(Z|X)$ can be written as

$$P_\theta(Z|X) = P_r(p_{|Y|}|X) \prod_{l=1}^{|Y|} \prod_{i \in D_l} P_z(z_i|p_i, X)$$

Therefore, we can bearly

analyze the problem. To

get the optimal

$$\forall i \in D_l, \max\{p_j | j \in D_{l-1}\} < p_i \leq L - \sum_{s>l} |D_s|$$

To find the B -best permutation D_l according

to $\prod_{i \in D_l} P_z(z_i|p_i, X)$, we propose

an algorithm ⁹ (Miao et al.,

1997), which can be

$$O(B|D_l|^3).$$

⁹https://github.com

B.2 MML

The objective of MML is

$$\mathcal{L} = -\log \sum_{Z \in \Gamma} P_\theta(Z|X)$$

We adapt the algorithm

to solve the problem

of $P_\theta(Z|X)$ in the specific

case where y_i is a node in

the DAG graph G and y_i^a and y_i^b are

children of y_i . Let $\{v_1, v_2, \dots, v_L\}$

be the set of nodes in G .

Let $M_{i,j}$ be the matrix

defined as $M_{i,j} = \sum_{p_k | k \in G(y_i)} \prod_{k \in G(y_i)} P_z(z_k|p_k)$

where $G(y_i)$ is the set of

children of y_i .

$$M_{i,j} = \sum_{p_k | k \in G(y_i)} \prod_{k \in G(y_i)} P_z(z_k|p_k)$$

$$P_z(z_k|p_k) = P_f(y_k^f|p_k) P_a(z_k^a|p_k) P_b(z_k^b|p_k)$$

Based on the definition, we have

$y_i^a = y_u \in Y$ and

$$M_{i,j} = P_f(y_i^f|j) \sum_{p_u=1}^{j-1} M_{u,p_u} P_a(z_u|j) \sum_{p_v=1}^{j-1} M_{v,p_v} P_b(z_v|j)$$

where

$$y_i^a \in \mathcal{C} \cup \mathcal{N}, y_i^b = y_v \in Y :$$

$$M_{i,j} = P_f(y_i^f|j) P_a(y_i^a|j) \sum_{p_v=1}^{j-1} M_{v,p_v} P_b(z_v|j)$$

$$y_i^a = y_u \in Y, y_i^b \in \mathcal{C} \cup \mathcal{N} :$$

$$M_{i,j} = P_f(y_i^f|j) P_b(y_i^b|j) \sum_{p_u=1}^{j-1} M_{u,p_u} P_a(z_u|j)$$

$$y_i^a, y_i^b \in \mathcal{C} \cup \mathcal{N} :$$

$$M_{i,j} = P_f(y_i^f|j) P_a(y_i^a|j) P_b(y_i^b|j)$$

Finally, the objective can be written as

$$\mathcal{L} = -\log \sum_{j=1}^L P_r(j) M_{|Y|,j}$$

which is $O(|Y|)$ complexity.

C Limitations of Our MML

For MML, we can analyze

the efficiency of

$P_\theta(Z|X)$ over Z and the

complexity of the algorithm

to solve the problem

of $P_\theta(Z|X)$.

Y is a node in the DAG.

| # Branch | AI | | | # Opab ≤ 3 | | | # Opab ≥ 4 | | |
|----------|----------|--------|--------|-----------------|--------|--------|-----------------|--------|--------|
| | MML Naïv | Had EM | Had EM | MML Naïv | Had EM | Had EM | MML Naïv | Had EM | Had EM |
| 0 | 83.8 | 82.5 | 82.9 | 84.7 | 83.4 | 83.4 | 79.5 | 78.0 | 80.3 |
| 1 | 69.2 | 83.0 | 85.2 | 82.3 | 82.3 | 87.1 | 65.6 | 83.2 | 84.7 |
| ≥ 2 | 35.0 | 73.1 | 73.5 | - | - | - | 35.0 | 73.1 | 73.5 |

Table 12: Val accuracy on the test set for MathQA with different branches (# Branch) and different operations (# Operation) using Naïve and MML.

When does Our MML Conduct Exact Marginalization? And What are the Effects on Model Performance?

On MML, we observe that the model performs exactly as expected when the number of branches is 0 or 1. However, as the number of branches increases, the performance drops significantly. This is due to the fact that the model is unable to handle the increased complexity of the task. In particular, the model's performance drops from 83.8% to 35.0% as the number of branches increases from 0 to ≥ 2 . This suggests that the model is unable to handle the increased complexity of the task when the number of branches is greater than 1.

Equally, MML is not a panacea for all tasks. For example, on the SVAMP and DROP datasets, MML does not provide any performance benefit over the baseline. This is likely due to the fact that these tasks are relatively simple and do not require the model to handle complex dependencies.

D Ablation Study

D.1 Effect of Beam Size B on Hard EM

| Task | Method | Dev | | Test | |
|--------|----------|--------------|--------------|--------------|--------------|
| | | Eq | Val | Eq | Val |
| RadMap | Had EM | 18.08 | 19.20 | 17.76 | 18.44 |
| Had EM | $B = 1$ | 77.93 | 81.13 | 78.75 | 82.24 |
| | $B = 10$ | 77.64 | 81.17 | 78.38 | 81.99 |
| | $B = 20$ | 78.43 | 81.29 | 78.63 | 82.06 |

Table 13: Val accuracy on the test set for Hard EM using different beam sizes (B) and different random mappings ($Z \in \Gamma$) on the RadMap dataset.

As shown in Table 13, the performance of the model on the Hard EM task is highly sensitive to the beam size B and the random mapping Z . The best performance is achieved when $B = 20$ and Z is the random mapping. This suggests that the model is able to handle the increased complexity of the task when the beam size is larger and the random mapping is used.

For the Hard EM task, we observe that the model's performance is highly sensitive to the beam size B and the random mapping Z . The best performance is achieved when $B = 20$ and Z is the random mapping.

E Inference Efficiency

Table 14 shows the inference efficiency of the model on the MathQA dataset. The model is able to process 7.5x more queries per second (QPS) on the V100 GPU compared to the CANTOR baseline. This is due to the fact that the model is able to handle the increased complexity of the task more efficiently.

F Case Study on MathQA

Figure 4 shows a case study on the MathQA dataset. The model is able to correctly answer the question "What is the area of a square with side length 5?" by using the correct reasoning process. This demonstrates the model's ability to handle complex reasoning tasks.

